Self-Modification of Spontaneous Emission by Inverse Opal Silica Photonic Crystals

Rick C. Schroden, Mohammed Al-Daous, and Andreas Stein*

Department of Chemistry, University of Minnesota, Minneapolis, Minnesota 55455

Received March 16, 2001. Revised Manuscript Received June 18, 2001

Modification of the photoluminescence emission of sol−gel-derived silica by three-dimensional photonic crystal effects is reported. Three-dimensionally ordered macroporous (3DOM) silica inverse opal materials prepared by polystyrene colloidal crystal templating, using the sol−gel method, exhibit broadband blue emission under UV excitation. 3DOM silica materials also possess a photonic stop band in the visible range of their optical spectra, with a controllable position dependent on several factors, including the macropore size, wall thickness, and refractive index contrast between the walls and the void-filling material. Tuning the photonic stop band of 3DOM silica to overlap with the photoluminescence emission band leads to competitive Bragg diffraction and electronic emission processes, resulting in a modified emission spectrum with a depression correlating with the spectral position of the stop band. Solvent-filling of the 3DOM silica changes the refractive index contrast and shifts the photonic stop band out of the spectral range of the photoluminescence emission band, restoring the broadband emission spectrum typical of sol−gel-derived silica. Grinding the 3DOM silica destroys the photonic crystal order, also restoring the broadband emission.

Introduction

In recent years, materials exhibiting a three-dimensional periodic modulation of the dielectric constant have received much attention, in both synthetic and theoretical fields. Such materials, first introduced by Yablonovitch and John, are known as photonic crystals.[1,2] Having a spatial periodicity with length scales on the order of optical wavelengths, photonic crystals behave with respect to electromagnetic waves in a manner analogous to the behavior of atomic crystals with electrons.[3] As an electronic band gap is created by the periodic arrangement of atoms in a semiconductor, the periodic electromagnetic modulation created by a photonic crystal can yield a gap of forbidden photon energies. When a very strong modulation of the refractive index (RI) is attained, a complete photonic band gap (PBG) occurs where Bragg diffractions simultaneously inhibit a range of wavelengths from propagating through the crystal for every state of polarization and propagation direction. For lower refractive index contrasts, incomplete photonic band gaps (i.e., stop bands) occur where a range of light wavelengths are partially inhibited from propagating in the material over certain directions. The motivation for the study of photonic crystals lies in the potential applications of photonic crystals exhibiting a complete PBG, which would allow for confinement and control of electromagnetic waves in all directions.[3−5] For example, photonic crystals could be used as optical waveguides with sharp bends,[6,7] as optical circuits,[7] as all-optical microchips,[8] and to inhibit the spontaneous emission from an excited chromophore, which may serve as a basis for thresholdless lasers.[1,9,10]

Two types of structures made by chemical methods that have been investigated as photonic crystals are synthetic opals,[11−16] which consist of monodisperse spherical particles with nm−μm scale diameters packed in a face-centered cubic arrangement, and inverse opals, formed by filling the void spaces of opal templates with a suitable structure-forming precursor and then removing the template to leave a three-dimensionally ordered

(1) Yablonovitch, E. *Phys. Rev. Lett.* **1987**, *58*, 2059−2062.
(2) John, S. *Phys. Rev. Lett.* **1987**, *58*, 2486-2489.
(3) Yablonovitch, E. *J. Opt. Soc. Am. B* **1993**, *10*, 283−295.
(4) Joannopoulos, J. D.; Villeneuve, P. R.; Fan, S. *Nature* **1997**, *386*, 143−149.
(5) Special Issue on Electromagnetic Crystal Structures, Design, Synthesis, and Application. *J. Lightwave Technol.* **1999**, *17*.
(6) Mekis, A.; Chen, J. C.; Kurland, I.; Fan, S.; Villeneuve, P. R.; Joannopoulos, J. D. *Phys. Rev. Lett.* **1996**, *77*, 3787−3790.
(7) Lin, S. Y.; Chow, E.; Hietala, V.; Villeneuve, P. R.; Joannopoulos, J. D. *Science* **1998**, *282*, 274−276.
(8) Chutinan, A.; Noda, S. *Appl. Phys. Lett.* **1999**, *75*, 3739.
(9) Yamamoto, Y.; Slusher, R. E. *Phys. Today* **1993**, *46*, 66−73.
(10) John, S. Theory of photonic band gap materials. In *Photonic Band Gap Materials*; Soukoulis, C. M., Ed.; Kluwer: Dordrecht, The Netherlands, 1996; pp 563−665.
(11) Bogomolov, V. N.; Gaponenko, S. V.; Kapitonov, A. M.; Prokofiev, A. V.; Ponyavina, A. N.; Silvanovich, N. I.; Samoilovich, S. M. *Appl. Phys. A* **1996**, *63*, 613−616.
(12) Bogomolov, V. N.; Gaponenko, S. V.; Germanenko, I. N.; Kapitonov, A. M.; Petrov, E. P.; Gaponenko, N. V.; Prokofiev, A. V.; Ponyavina, A. N.; Silvanovich, N. I.; Samoilovich, S. M. *Phys. Rev. E* **1997**, *55*, 7619−7625.
(13) Mayoral, R.; Requena, J.; Moya, J. S.; López, C.; Cintas, A.; Míguez, H.; Meseguer, F.; Vázquez, L.; Holgado, M.; Blanco, A. *Adv. Mater.* **1997**, *9*, 257−260.
(14) Míguez, H.; López, C.; Meseguer, F.; Blanco, A.; Vázquez, L.; Mayoral, R.; Ocaña, M.; Fornés, V.; Mifsud, A. *Appl. Phys. Lett.* **1997**, *71*, 1148.
(15) Romanov, S. G.; Johnson, N. P.; Fokin, A. V.; Butko, V. Y.; Yates, H. M.; Pemble, M. E.; Sotomayor Torres, C. M. *Appl. Phys. Lett.* **1997**, *70*, 2091.
(16) Vlasov, Y. A.; Astratov, V. N.; Karimov, O. Z.; Kaplyanskii, A. A.; Bogomolov, V. N.; Prokofiev, A. V. *Phys. Rev. B* **1997**, *55*, R13357−R13360.

10.1021/cm010230s CCC: $20.00
Published on Web 08/07/2001

macroporous (3DOM) material.[17−22] Several studies have reported modification of the spontaneous emission from luminescent species embedded in photonic crystals, including organic dyes embedded in silica[12,23−26] and latex opals[27,28] and in titania inverse opals,[29] semiconductors embedded in silica[26,30,31] and latex opals,[32−34] and intrinsic oxygen defects[31] and rare earth ions[26,35] in silica opals. While the modulation of the refractive index in these materials was not large enough to produce a complete PBG, significant modification of the emission spectra occurred when the photonic stop band overlapped the emission band.

In the current study, the light-emitting species is sol−gel-derived silica. Pure silica materials are immune to electrooptical activity. However, silica prepared by the sol−gel method, which involves hydrolysis and condensation of alkoxysilanes, exhibits broadband blue photoluminescence (PL) centered at approximately 440 nm upon UV irradiation that persists for several seconds after removal of the source. The origin of PL in sol−gel-derived silica has been attributed to both oxygen defect centers in the −O−Si−O− network[36−40] and to carbon impurities incorporated within the silica network.[41−44] In the present study, 3DOM silica inverse opal materials (shown in Figure 1) were prepared by an optimized version of the sol−gel process using the polystyrene (PS) colloidal crystal templating technique.[18,20] Here we report the effect of the photonic stop band of 3DOM silica inverse opal materials on their PL emission spectra. Results are compared for a 3DOM silica sample with a photonic stop band that overlaps with the PL emission band and for a macroporous silica sample without overlap of the bands. Significant modification of the PL emission band was observed for the 3DOM silica material with an overlapping photonic stop band, resulting in a depression correlating with the spectral position of the stop band. Removal of the photonic stop band from the PL emission band region was explored by two methods, and the results are discussed. In the first approach, the 3DOM silica material was filled with solvent, which changes the refractive index contrast between the silica walls and voids, resulting in a shift in the stop band position. In the second approach, the regular three-dimensional order was removed by physically grinding the material to destroy the photonic crystal effect. Both techniques led to the restoration of the typical broadband emission spectrum of sol−gel-derived silica.

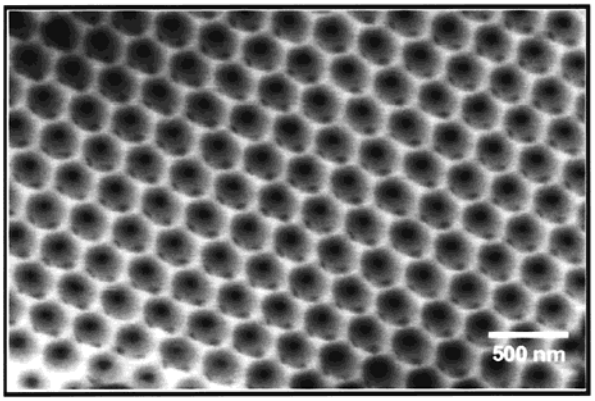

Figure 1. Scanning electron micrograph (SEM) of a three-dimensionally ordered macroporous (3DOM) silica inverse opal material, showing a regular arrangement of macropores (gray regions) connected by smaller windows (black regions).

Experimental Section

Materials. Reagents were obtained from the following sources: tetramethoxysilane (TMOS), HCl (37%), and methyl methacrylate were from Aldrich; absolute ethanol was from Aaper Alcohol and Chemical Co.; methanol was from Pharmcoproducts Inc.; and styrene was from Mallinckrodt. All chemicals were used as received without further purification. Water used in all syntheses was distilled and deionized to 17.7 MΩ cm. Monodisperse polystyrene (PS) and poly(methyl methacrylate) (PMMA) spheres were prepared by surfactant-free emulsion polymerization and packed into colloidal crystals by centrifugation as described previously.[18,20,22] 3DOM silica materials were prepared by an optimized version of the sol−gel process previously reported,[18,20] using colloidal crystal PS as the template. 3DOM magnesium oxide was prepared with a PMMA template according to literature methods.[45]

Synthesis and Characterization of 3DOM Silica. *Synthesis.* 3DOM SiO_2 was synthesized from mixtures of typical composition: 4.0 mL of TMOS, 2.0 mL of methanol, and 0.4

(17) Velev, O. D.; Jede, T. A.; Lobo, R. F.; Lenhoff, A. M. *Nature* **1997**, *389*, 447−448.
(18) Holland, B. T.; Blanford, C. F.; Stein, A. *Science* **1998**, *281*, 538−540.
(19) Wijnhoven, J. E. G. J.; Vos, W. L. *Science* **1998**, *281*, 802−804.
(20) Holland, B. T.; Blanford, C. F.; Do, T.; Stein, A. *Chem. Mater.* **1999**, *11*, 795−805.
(21) Blanco, A.; Chomski, E.; Grabtchak, S.; Ibisate, M.; John, S.; Leonard, S. W.; Lopez, C.; Meseguer, F.; Miguez, H.; Mondia, J. P.; Ozin, G. A.; Toader, O.; van Driel, H. M. *Nature* **2000**, *405*, 437−440.
(22) Yan, H.; Blanford, C. F.; Smyrl, W. H.; Stein, A. *Chem. Commun.* **2000**, *16*, 1477−1478, and references therein.
(23) Petrov, E. P.; Bogomolov, V. N.; Kalosha, I. I.; Gaponenko, S. V. *Phys. Rev. Lett.* **1998**, *81*, 77−80.
(24) Megens, M.; Wijnhoven, J. E. G. J.; Lagendijk, A.; Vos, W. L. *J. Opt. Soc. Am. B* **1999**, *16*, 1403−1408.
(25) Romanov, S. G.; Maka, T.; Torres, C. M. S.; Müller, M.; Zentel, R. *J. Lightwave Technol.* **1999**, *17*, 2121−2127, and references therein.
(26) Gaponenko, S. V.; Bogomolov, V. N.; Petrov, E. P.; Kapitonov, A. M.; Yarotsky, D. A.; Kalosha, I. I.; Eychmueller, A. A.; Rogach, A. L.; McGilp, J.; Woggon, U.; Gindele, F. *J. Lightwave Technol.* **1999**, *17*, 2128−2137.
(27) Park, S. H.; Gates, B.; Xia, Y. *Adv. Mater.* **1999**, *11*, 462−466.
(28) Müller, M.; Zentel, R.; Maka, T.; Romanov, S. G.; Sotomayor Torres, C. M. *Chem. Mater.* **2000**, *12*, 2508−2512.
(29) Schriemer, H. P.; van Driel, H. M.; Koenderink, A. F.; Vos, W. L. *Phys. Rev. A* **2000**, *63*, 011801(R).
(30) Blanco, A.; López, C.; Mayoral, R.; Míguez, H.; Meseguer, F. *Appl. Phys. Lett.* **1998**, *73*, 1781−1783.
(31) Romanov, S. G.; Fokin, A. V.; De La Rue, R. M. *Appl. Phys. Lett.* **1999**, *74*, 1821−1823.
(32) Rogach, A.; Susha, A.; Caruso, F.; Sukhorukov, G.; Kornowski, A.; Kershaw, S.; Möhwald, H.; Eychmüller, A.; Weller, H. *Adv. Mater.* **2000**, *12*, 333−337.
(33) Zhou, J.; Zhou, Y.; Buddhudu, S.; Ng, S. L.; Lam, Y. L.; Kam, C. H. *Appl. Phys. Lett.* **2000**, *76*, 3513−3515.
(34) Rogach, A. L.; Kotov, N. A.; Koktysh, D. S.; Ostrander, J. W.; Ragoisha, G. A. *Chem. Mater.* **2000**, *12*, 2721−2726.
(35) Romanov, S. G.; Fokin, A. V.; De La Rue, R. M. *Appl. Phys. Lett.* **2000**, *76*, 1656−1658.
(36) Yoldas, B. E. *J. Mater. Res.* **1990**, *5*, 1157−1158.
(37) Bertino, M.; Corazza, A.; Martini, M.; Mervic, A.; Spinolo, G. *J. Phys.: Condens. Matter* **1994**, *6*, 6345−6352.
(38) Ayers, M. R.; Hunt, A. J. *J. Non-Cryst. Solids* **1997**, *217*, 229−235.
(39) Kalceff, M. A. S. *Phys. Rev. B* **1997**, *57*, 5674−5683.
(40) Meinardi, F.; Paleari, A. *Phys. Rev. B* **1998**, *58*, 3511−3514.
(41) Canham, L. T.; Loni, A.; Calcott, P. D. J.; Simons, A. J.; Reeves, C.; Houlton, M. R.; Newey, J. P.; Nash, K. J.; Cox, T. I. *Thin Solid Films* **1996**, *276*, 112−115.
(42) Green, W. H.; Le, K. P.; Grey, J.; Au, T. T.; Sailor, M. J. *Science* **1997**, *276*, 1826−1828.
(43) Bekiari, V.; Lianos, P. *Langmuir* **1998**, *14*, 3459−3461, and references therein.
(44) Bekiari, V.; Lianos, P. *Chem. Mater.* **1998**, *10*, 3777−3779.
(45) Yan, H.; Blanford, C. F.; Holland, B. T.; Smyrl, W. H.; Stein, A. *Chem. Mater.* **2000**, *12*, 1134−1141.

mL of HCl. Methanol was mixed with TMOS in a small vial at room temperature. HCl was added and the sample was stirred for 3 min. The solution was then applied dropwise to completely cover millimeter-thick layers of dried PS sphere colloidal crystals, which were crushed and deposited on filter paper in a Büchner funnel with suction applied. The composite sample was allowed to dry in air at room temperature for 24 h. PS was removed from the sample by calcination in air at 550 °C for 10 h. The pore diameters of the 3DOM silica samples were tailored to produce one sample with 283 nm pores, SiO_2-(283), which had an overlap of the stop band with the emission band, and another reference sample with 386 nm pores, SiO_2-(386), with no overlap, by choice of PS sphere size. PS spheres used in the syntheses had average diameters of 325 ± 5 and 456 ± 10 nm for SiO_2(283) and SiO_2(386), respectively.

Elemental Analysis. Despite calcination at 550 °C, small amounts of carbon impurities remained in the samples. Carbon content (wt %) was 0.68% for SiO_2(283) and 0.37% for SiO_2-(386).

IR Spectra. The IR spectra of the as-synthesized 3DOM silica materials were dominated by PS absorptions. Calcination removed nearly all bands due to PS; however, two very weak absorptions remained at 2925 and 2855 cm^{-1}, which can be attributed to hydrocarbon impurities in the samples. The spectra were dominated by intense and broad stretching vibrations at ca. 1100 cm^{-1} [ν_{asym}(Si−O−Si)] and 810 cm^{-1} [ν_{sym}-(Si−O−Si)] and bending vibration at 465 cm^{-1} [δ(Si−O−Si)].[46]

Scanning Electron Microscopy (SEM). Sphere size, macropore size, and extent of ordering of the products were determined using SEM. The average pore spacings were 283 ± 5 and 386 ± 15 nm for SiO_2(283) and SiO_2(386), respectively. SiO_2(283) was vigorously ground using a mortar and pestle to destroy the regular periodic order, and the progress was monitored by SEM.

Diffuse-Reflectance (DR) UV−vis Spectroscopy. Spectra were obtained for randomly oriented bulk powder samples. Reflectance data were converted to $f(R_\infty)$ values using the Kubelka−Munk equation. Reflections (stop bands) corresponding to (111) planes were observed for 3DOM silica filled with air and solvents. Reflections corresponding to (220) planes were only observed for solvent-filled samples. Observed central position of reflections (and corresponding planes): SiO_2(386), 668 nm (111); SiO_2(283), 492 nm (111); SiO_2(283) filled with ethanol, 634 nm (111), 392 nm (220).

Luminescence Spectrometry. Emission spectra were obtained for bulk powder samples, with constant excitation at 365 nm. Variations in the density of bulk samples in the cuvette were found to affect the intensity, but not the shape, of the emission band. Photoluminescence quantum yield measurements were made according to published techniques.[43]

Instrumentation Details. Elemental analysis was performed for C and H at Atlantic Microlab Inc., Norcross, GA. Infrared spectroscopy was performed on a Nicolet Magna-IR 760 spectrometer with mid-IR and far-IR capability. Spectra were obtained using the powdered samples in FT-IR grade KBr pellets. SEM images were obtained on a Hitachi S-800 scanning electron microscope operating at 5 kV. Samples for SEM were dusted on an adhesive conductive carbon disk attached to an aluminum mount and were coated with Pt prior to examination. Diffuse reflectance UV−vis spectra were obtained on a Hewlett-Packard 8452A diode array spectrophotometer equipped with a Labsphere RSA-HP-84 reflectance spectroscopy accessory. Photoluminescence emission spectra were obtained using a Perkin-Elmer LS 50B luminescence spectrometer.

Results and Discussion

Photoluminescence of 3DOM Silica. The 3DOM silica materials studied here displayed visible photoluminescence upon UV irradiation, with typical quantum yields of 22%. To investigate the influence of a photonic stop band on the photoluminescence (PL) spectra of the 3DOM silica materials, samples were chosen for which the stop band overlaps with the PL emission band, SiO_2-(283), and for which the bands do not overlap, SiO_2(386). Excitation at 365 nm produced the emission spectra for SiO_2(283) and SiO_2(386) shown in Figure 2. The spectrum of SiO_2(283) is given on expanded (Figure 2A) and normalized (Figure 2B) intensity scales for easier visualization of peak shapes and relative intensities. In the normalized case (Figure 2B), the intensity values were scaled to overlay the high-wavelength edges of the spectra for SiO_2(283) and SiO_2(386). The emission spectrum of SiO_2(386) (Figure 2C) displays a broad, featureless bell-shaped band, which is typical for sol−gel derived silica. In contrast, the emission spectrum of SiO_2(283) displays a dip in the low-wavelength region. The origin of this dip can be explained by an overlap of the emission spectrum with the stop band of SiO_2(283). The diffuse-reflectance (DR) UV−vis spectrum of SiO_2-(283), shown in Figure 2D, reveals a broad photonic stop band centered at 492 nm [due to Bragg diffraction from the (111) planes of the fcc structure] comparable to the width of the emission band. The relative width of the stop band is approximately 15% (a normalized measure of the photonic stop band given by the ratio of the width at half-height to the central position of the dip). The stop bands of 3DOM silica inverse opals are much wider than those observed for normal opal (ca. 6%),[31,35] allowing 3DOM materials to suppress emission over a larger spectral range. Comparison of the DR UV−vis (Figure

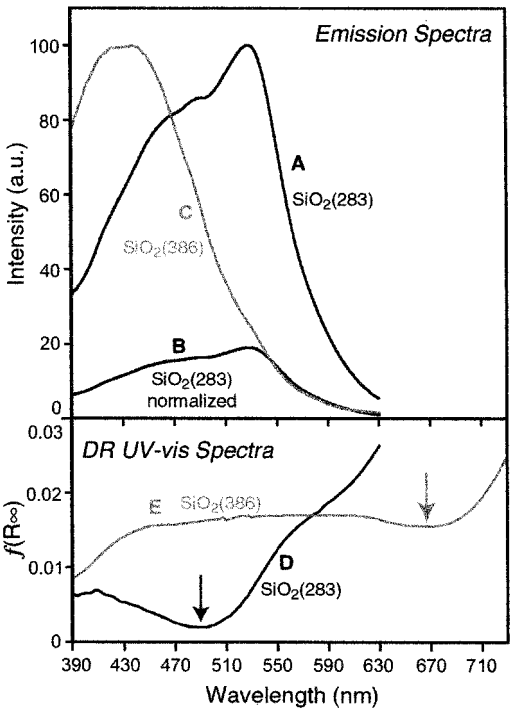

Figure 2. Photoluminescence (PL) emission spectra of SiO_2-(283) with expanded (A) and normalized (B) intensity scales. (C) PL emission spectrum of SiO_2(386). Excitation wavelength = 365 nm. Diffuse reflectance (DR) UV−vis spectra of (D) SiO_2-(283) and (E) SiO_2(386) with stop bands marked by arrows. Modification of the spontaneous emission of the silica skeleton is observed for SiO_2(283) due to overlap of the PL emission band with the photonic stop band.

(46) Brinker, C. J.; Scherer, G. W. *Sol−Gel Science: the Physics and Chemistry of Sol−Gel Processing*; Academic Press: San Diego, 1990.

2D) and PL emission (Figure 2A,B) spectra of SiO_2(283) shows that the depression in the emission spectrum corresponds to the spectral position of the stop band. The emission intensity decreases where an overlap of the stop band occurs. Since the stop band of SiO_2(386) (Figure 2E) lies outside of the range of the emission band, the PL spectrum is unaffected by the 3DOM order. Assuming similar emission processes, it may be concluded that photonic crystal effects are responsible for the difference in the PL spectra of the two silica samples.

Infiltration of 3DOM Silica with Solvent. By filling the voids of 3DOM silica with a solvent, the position of the stop band can be predictably altered.[47] An approximate expression for the position of the stop band is given by a modified version of Bragg's law, combined with Snell's law to account for the reduced angle with respect to the normal that light travels upon entering the inverse opal:

$$\lambda = \frac{2d_{hkl}}{m}\sqrt{n^2_{\text{avg}} - \sin^2\theta} \qquad (1)$$

where λ is the wavelength of the stop band minimum, d_{hkl} is the interplanar spacing, m is the order of Bragg diffraction, n_{avg} is the average refractive index of the material, and θ is the angle measured from the normal to the planes. Since the DR UV−vis measurements were made on bulk, randomly oriented samples, the spectra display minima at the calculated value for normal incidence ($\theta = 0°$), and the angle-dependent term can be dropped from the equation:

$$\lambda = \frac{2d_{hkl}}{m}n_{\text{avg}} \qquad (2)$$

Using the effective medium approximation,[25] the average RI of the material can be calculated by a weighted sum of the components:

$$n_{\text{avg}} = \sum n_i\phi_i \qquad (3)$$

where n_i and ϕ_i are the RI and volume fraction of the ith component. Applying this relation to eq 2 gives an expression for the position of the stop band for a filled inverse opal:

$$\lambda = \frac{2d_{hkl}}{m}[\phi\, n_{\text{wall}} + (1-\phi)n_{\text{void}}] \qquad (4)$$

where ϕ is the solid fraction of the material. For an fcc lattice with unit cell parameter a, the interplanar spacing d_{hkl} is given by

$$d_{hkl} = \frac{a}{\sqrt{h^2+k^2+l^2}} \qquad (5)$$

and the pore spacing D is given by

$$D = \frac{a}{\sqrt{2}} \qquad (6)$$

(47) Blanford, C. F.; Schroden, R. C.; Al-Daous, M.; Stein, A. *Adv. Mater.* **2001**, *13*, 26−29, and references therein.

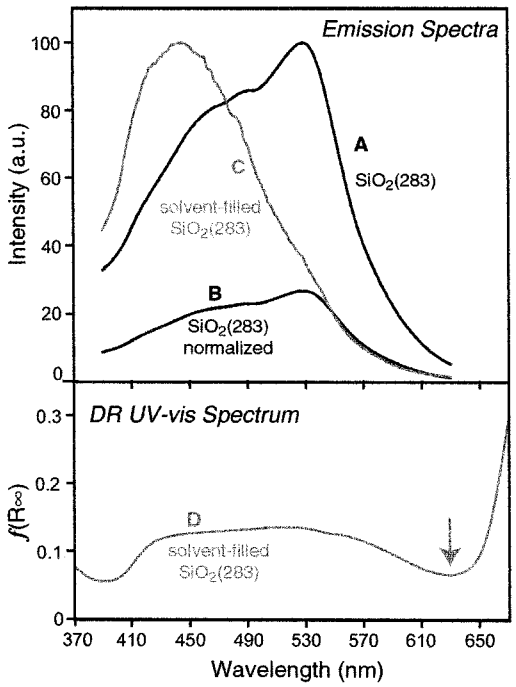

Figure 3. PL emission spectra of SiO_2(283) with expanded (A) and normalized (B) intensity scales. (C) PL emission spectrum of SiO_2(283) with its voids filled with ethanol. Excitation wavelength = 365 nm. (D) DR UV−vis spectrum of SiO_2(283) filled with ethanol. Filling with ethanol shifts the photonic stop band (marked with an arrow) of SiO_2(283) to a region where it no longer overlaps with the PL emission band, restoring the bell-shaped spectrum.

To confirm that the dip in the emission spectrum of SiO_2(283) is indeed due to photonic crystal effects, the effect of solvent-filling of the 3DOM silica voids on the emission spectrum was studied. Upon filling SiO_2(283) with ethanol, stop bands corresponding to Bragg diffractions from the (111) and (220) sets of planes are expected to be observed in the visible spectrum. The predicted positions of the stop band minima for air- and ethanol-filled SiO_2(283) can be calculated using eq 4 (from the measured pore spacing D = 283 nm; approximate filling fraction ϕ = 14%; known RI values $n_{SiO_2} = 1.455$, $n_{\text{air}} = 1.000$, and $n_{\text{ethanol}} = 1.360$; and first-order Bragg diffraction m = 1). The calculated (and observed) stop band positions are 492 nm (492 nm), 635 nm (634 nm), and 389 nm (392 nm) for reflections from the (111) planes of SiO_2(283) filled with air and the (111) and (220) planes of SiO_2(283) filled with ethanol, respectively. It is notable that the shift in the stop band position upon filling 3DOM silica inverse opals with solvent is more than three times greater than that observed for normal opals,[11,12] due to the smaller solid fraction in the 3DOM materials. The emission spectra of SiO_2(283) and SiO_2(283) filled with ethanol and the DR UV−vis spectrum of SiO_2(283) filled with ethanol are shown in Figure 3. The spectrum of SiO_2(283) is given on expanded (Figure 3A) and normalized (Figure 3B) intensity scales, with the intensity values for the normalized SiO_2(283) spectrum scaled to overlay the high-wavelength edge of the spectrum of solvent-filled SiO_2(283). By filling the voids of SiO_2(283) with ethanol, the stop band corresponding to diffraction from the (111) planes shifted from 492 to 634 nm, where it no longer overlapped with the emission spectrum. The result was

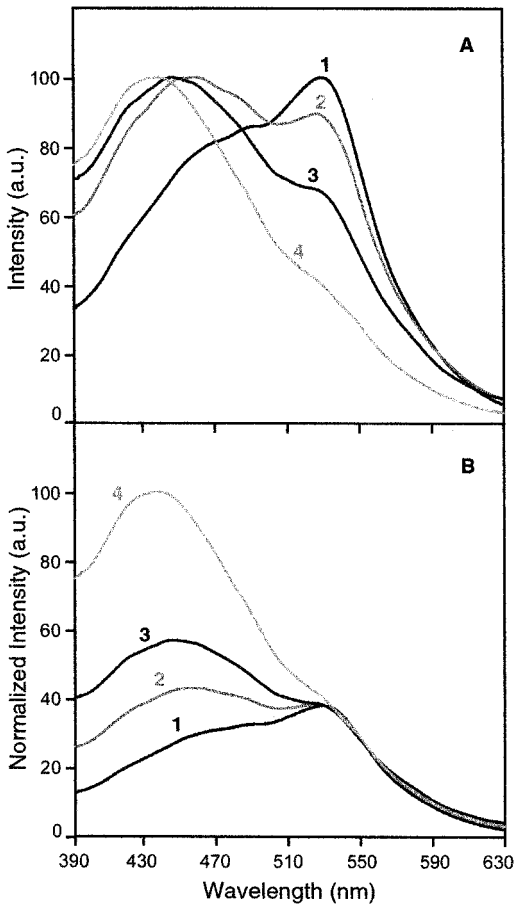

Figure 4. PL emission spectra with expanded (A) and normalized (B) intensity scales of SiO_2(283) initially (1) and after three stages of grinding the sample to remove the photonic crystal structure, progressing from spectrum 2 to 4. Excitation wavelength = 365 nm. With increased grinding the low-wavelength intensity of the emission band recovers as the photonic stop band effect is lost.

a restoration of the bell-shaped emission spectrum, confirming that photonic crystal effects are responsible for the dip in the PL emission band of SiO_2(283).

Effect of Grinding the 3DOM Silica. The influence of the photonic stop band of SiO_2(283) on its PL emission spectrum was investigated directly by grinding the sample to destroy the regular three-dimensional order. This process allows for comparison of the emission spectra of the same sample in ordered and disordered states, assuming similar photoluminescence emission processes in both states. The emission spectra of original SiO_2(283) and crushed SiO_2(283) samples are shown in parts A and B of Figure 4, with peaks scaled to the same height, and on a normalized intensity scale for easier visualization of peak shapes and relative intensities. Spectrum 1 was obtained for original SiO_2(283). Spectra 2−4 were acquired after increasing amounts of grinding the sample to destroy the photonic crystal order. Comparison of the spectra shows that the modified band of SiO_2(283) was restored to the typical bell-shaped band upon grinding, making it apparent that the photonic crystal structure was responsible for the depression observed in the PL emission spectrum of SiO_2(283). It can be seen from Figure 4B that the photonic crystal structure of SiO_2(283) significantly suppressed emission from the sample over a wide spectral range.

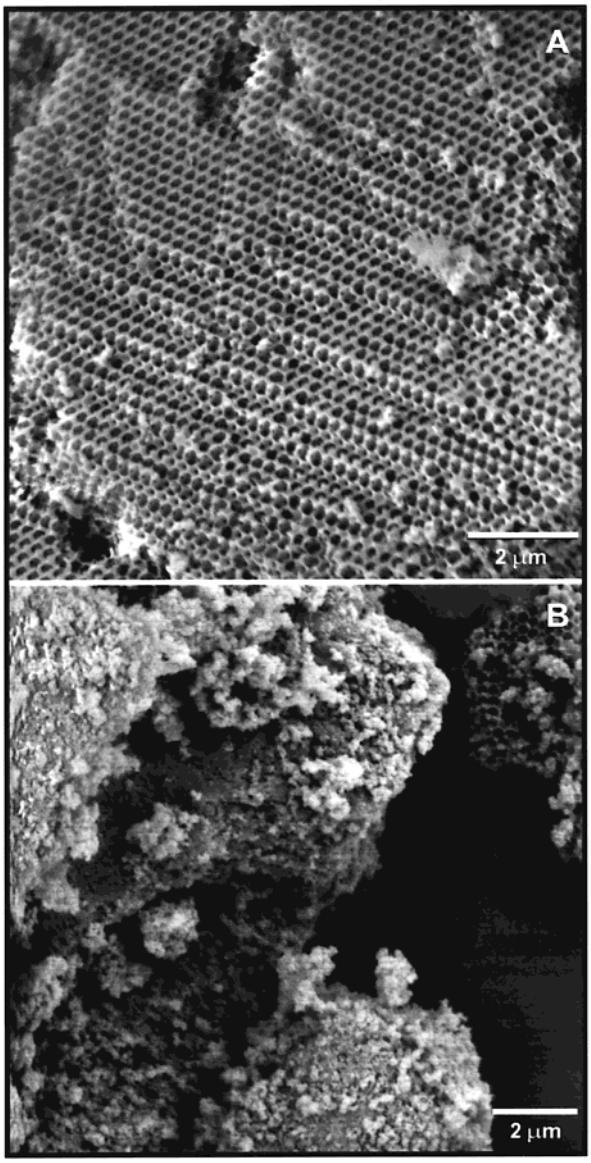

Figure 5. SEM images comparing (A) SiO_2(283) with regular three-dimensional order and (B) SiO_2(283) after the final stage of grinding has removed most of the order. Some small ordered domains remain; however, the majority of the material is disordered.

SEM images of SiO_2(283) originally and after the final stage of grinding are given in Figure 5. The image of SiO_2(283) displays the regular periodic order that is responsible for its photonic crystal behavior. The crushed sample maintains some macroporosity; however, it has become significantly disordered to remove the photonic crystal behavior of the bulk material. These results confirm the photonic crystal origin of the observed depression in the PL emission spectrum of SiO_2(283). A comparison of the PL emission spectra of the reference sample SiO_2(386) (with no stop band/emission band overlap; Figure 6A) to spectra of SiO_2(283) in which the overlapping photonic stop band has been removed by grinding the sample (Figure 6B) and solvent-filling of the voids (Figure 6C) is given in Figure 6. Both processes lead to emission spectra similar to that of SiO_2(386). The reduced intensity of the emission band for solvent-filled SiO_2(283) (Figure 6C) in the low wavelength region may be due to partial overlap with the (220) stop band.

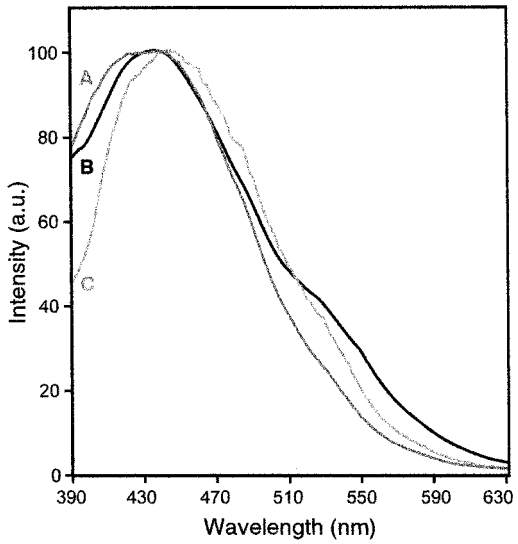

Figure 6. PL emission spectra of (A) SiO_2(386), (B) crushed SiO_2(283), and (C) SiO_2(283) filled with ethanol. Crushing or filling with ethanol removes the stop band of SiO_2(283) from overlapping with the emission band, restoring the typical broadband spectra similar to SiO_2(386) (which does not have overlapping stop and emission bands).

Conclusion

The effect of a photonic stop band on the photoluminescence emission spectrum of sol−gel derived silica has been investigated. 3DOM silica samples were tailored to give one sample with an overlap of the stop band with the emission band and another reference sample with no overlap. The emission spectra of the two samples differed; it was found that the photonic stop band modified the emission band in the spectral region where overlap occurred, producing a depression in the emission band corresponding to the stop band position. The photonic crystal origin of the modified emission spectrum was tested by solvent-filling of the voids to shift the position of the stop band out of the spectral range of the emission and by crushing the sample to destroy the regular periodic order. Both stop band modification techniques restored the broad bell-shaped emission band typical of sol−gel-derived silica, confirming that photonic crystal effects were responsible for the dip in the emission spectrum.

Photonic crystals of 3DOM silica inverse opals allow for suppression of emission over a much larger spectral range than normal opals due to their wider stop bands, and they exhibit a greater response in the stop band shift upon solvent-filling due to the smaller solid fraction of 3DOM materials. While the refractive index contrast in the 3DOM silica materials studied here was not sufficient to produce a complete photonic band gap, the fundamental concept of suppressed spontaneous emission is important for the realization of thresholdless lasers and other photonic devices.[1,3,9,10] The flexibility of the latex sphere templating approach allows for the preparation of a large range of compositions,[17−22] which may potentially be tailored to produce competitive Bragg diffraction and electronic emission processes. Preliminary investigations suggest that similar modified emission characteristics can be obtained for 3DOM compositions with a higher refractive index than silica, as sol−gel-derived alumina, zirconia,[36] and macroporous magnesium oxide[48] exhibit similar visible photoluminescence upon UV excitation.

Acknowledgment. We thank the David and Lucile Packard Foundation, 3M, DuPont, the National Science Foundation (DMR-9701507), and the MRSEC program of the NSF under award number DMR-9809364 for support of this research. We thank David Blank for helpful discussions.

CM010230S

(48) Schroden, R. C.; Yan, H.; Stein, A. *unpublished work* **2001**.